Published in final edited form as:
J Geriatr Psychiatry Neurol. 2010 September ; 23(3): 185–198. doi:10.1177/0891988710363715.

Pittsburgh Compound B (^{11}C-PIB) and fluorodeoxyglucose (^{18}F-FDG) PET in Patients with Alzheimer's Disease, Mild Cognitive Impairment, and Healthy Controls

D. P. Devanand, MD[1,3,4], **Arthur Mikhno, B.S.**[2,4], **Gregory H. Pelton, MD**[1,3,4], **Katrina Cuasay, BS**[1,3,4], **Gnanavalli Pradhaban, MBBS**[1,3,4], **J.S. Dileep Kumar, PhD**[2,3,4], **Neil Upton, PhD**[6], **Robert Lai, MD**[6], **Roger N. Gunn, PhD**[5], **V. Libri, MD**[6], **Xinhua Liu, PhD**[7], **Ronald van Heertum, MD**[4,8], **J. John Mann, MD**[2,3,4], and **Ramin V. Parsey, MD, PhD**[2,3,4]

[1]Division of Geriatric Psychiatry, Columbia University, New York, U.S.A.

[2]Division of Molecular Imaging and Neuropathology, Columbia University, New York, U.S.A.

[3]New York State Psychiatric Institute, Columbia University, New York, U.S.A.

[4]College of Physicians and Surgeons, Columbia University, New York, U.S.A.

[5]GlaxoSmithKline CIC, Essex, United Kingdom

[6]Neurosciences-CEDD, Essex, United Kingdom

[7]Department of Biostatistics, School of Public Health, Columbia University, New York, USA

[8]Department of Radiology, College of Physicians and Surgeons, Columbia University, New York, USA

Abstract

Amyloid load in the brain using ^{11}C-PIB PET and cerebral glucose metabolism using ^{18}F-FDG PET were evaluated in patients with mild Alzheimer's disease (AD, n=18), mild cognitive impairment (MCI, n=24) and controls (CTR, n=18). ^{11}C-PIB binding potential (BP_{ND}) was higher in prefrontal cortex, cingulate, parietal cortex, and precuneus in AD compared to CTR or MCI, and in prefrontal cortex for MCI compared to CTR. For ^{18}F-FDG, rCMRGlu was decreased in precuneus and parietal cortex in AD compared to CTR and MCI, with no MCI-CTR differences. For the AD-CTR comparison, precuneus BP_{ND} area under the ROC curve (AUC) was 0.938 and parietal cortex rCMRGlu AUC was 0.915; for the combination AUC was 0.989. ^{11}C-PIB PET BP_{ND} clearly distinguished diagnostic groups, and combined with ^{18}F-FDG PET rCMRGlu this effect was stronger. These PET techniques provide complementary information in strongly distinguishing diagnostic groups in cross-sectional comparisons that need testing in longitudinal studies.

Keywords

Alzheimer's disease; mild cognitive impairment; PET scan; Pittsburgh Compound B; FDG

For correspondence contact: D.P. Devanand, M.D., 1051 Riverside Drive, Unit 126, New York, NY 10032. dpd3@columbia.edu, Phone: 212-543-5612, Fax: 212-543-5854.

Disclosure Statement

Drs. Gunn, Libri, Lai and Upton are GSK employees and report owning shares in GSK but declare that they have no financial interest in or financial conflict with the subject matter or materials discussed in this article. Dr. Devanand has received research support from Novartis and Eli Lilly, and has served as a consultant to GSK, Bristol Myers Squibb, and Sanofi-Aventis. Dr. Mann has received research support from GSK and Novartis. Dr. Parsey has received research support from GSK, Novartis, and Sepracor.

INTRODUCTION

Alzheimer's disease (AD) accounts for 60–70% of cases of dementia with an estimated 4.5 million people with AD in the United States[1]. The clinical diagnosis of AD has an estimated sensitivity of 68% to 100% and specificity of 65 to 91% when compared to gold standard neuropathological diagnosis that relies on the presence and abundance of extracellular amyloid (Aβ) plaques and intracellular neurofibrillary tangles (NFTs) [2]. Clinical symptoms likely appear after significant deposition of amyloid has already occurred[3], and amyloid deposition begins several years before clinical symptoms of dementia develop [4, 5].

N-methyl-^{11}C-2-(4-methylaminophenyl)-6-hydroxybenzothiazole (also known as ^{11}C-6-OH-BTA-1 or ^{11}C-PIB) is an amyloid-binding positron emission tomography (PET) tracer. ^{11}C-PIB binds to fibrillar amyloid with no detectable binding to soluble Aβ forms or neurofibrillary tangles under PET study conditions[6]. Regional ^{11}C-PIB binding correlates with amyloid plaques and vascular amyloid at autopsy[7, 8].

In clinical studies, compared to healthy control subjects, patients with AD have higher ^{11}C-PIB binding in the prefrontal, precuneus, parietal and cingulate regions, with the least binding differences in the medial temporal lobe, visual, sensory and motor cortex[3, 9,10,11,12]. Some control subjects also show increased binding [9,10,13], which may herald a future diagnosis of AD[10,14]. Less work has been done with ^{11}C-PIB in patients with mild cognitive impairment (MCI), which is associated with an increased likelihood of conversion to AD. ^{11}C-PIB studies in small samples suggest that approximately two-thirds of amnestic MCI patients show ^{11}C-PIB retention similar to AD, while one-third are in the healthy control range[9,15,16,17,18]. In MCI, amyloid positive ^{11}C-PIB PET may indicate an increased likelihood of conversion to AD[19].

An older, more widely available technique is ^{18}F-FDG PET. Relative hypometabolism in the parietotemporal and posterior cingulate regions characterizes patients with AD and distinguishes them from healthy controls, though it may not be highly specific to AD [20,21]. ^{18}F-FDG PET studies in small samples of MCI patients show that parietotemporal and posterior cingulate hypometabolism may characterize future converters to AD [22, 23].

As summarized in Table 1, there is growing, but still limited, published data on the comparative and conjoint use of ^{11}C-PIB PET and ^{18}F-FDG PET in elderly cognitively impaired subjects [3,11,24]. To examine the degree to which these PET tracers, individually and combined, distinguish patients with mild AD, MCI, and healthy age-matched control subjects (CTR), we conducted a PET study using ^{11}C-PIB and ^{18}F-FDG PET.

METHODS

Subjects

MCI and mild AD patients presented with memory complaints to a Memory Disorders Center at New York State Psychiatric Institute/Columbia University. Based on consensus diagnosis, AD patients met National Institute of Neurological and Communicative Diseases and Stroke/Alzheimer's Disease and Related Disorders Association (NINCDS-ADRDA) criteria for probable AD[25]. Folstein Mini Mental State Exam (MMSE) > 16 was required for study inclusion. In MCI and CTR, a neuropsychological test battery was administered. This comprised the MMSE, SRT (12-item, 6-trial Selective Reminding Test), Wechsler Memory Scale (WMS) Visual Reproduction Test, Category Fluency (Animal Naming and Letter Fluency), Boston Naming 60-item, BDAE sentence repetition and comprehension, WAIS-R similarities, digit symbol and block design, and the Alzheimer's Disease Assessment Scale

(ADAS-cog). AD patients received only the MMSE, SRT and ADAS-cog, and hence only these three cognitive measures were evaluated in analyses.

Amnestic MCI was diagnosed by Petersen criteria[26] requiring subjective memory complaints and either SRT immediate or delayed recall scores greater than 1.5 SD below age and education adjusted norms in the absence of impairment in activities of daily living. Non-amnestic MCI patients were required to score > 1.5 SD below norms on any non-memory test and meet the same clinical criteria. All controls were required to have MMSE ≥ 27 with recall ≥ 2 of 3 objects at 5 minutes, SRT total and delayed recall scores within 1 SD of age-adjusted norms, and not have a current diagnosis of any DSM-IV Axis I psychiatric disorder, neurological disorder, or acute medical illness. Family history of dementia was not an exclusion criterion. Subjects receiving Warfarin were excluded, as were all subjects with any contraindication to MRI or PET imaging. Controls were group-matched to patients on age and sex. Five healthy controls were recruited by advertisement (out of 21 subjects who passed a telephone screen and then had in-person evaluation and testing) and 13 controls were recruited during their participation in a long-term follow-up study in the clinic. All participants signed informed consent in this IRB-approved protocol.

^{11}C-PIB Synthesis

The full radiosynthesis of [N-Methyl ^{11}C]-2-(4-methylaminophenyl)-6-hydroxybenzothiazole ([^{11}C]-6-OH-BTA-1) is described elsewhere[27]. The average yield was found to be 14.5% at End of Synthesis with a specific activity > 37 GBq/ μmol.

PET Imaging

Head movement was minimized using a polyurethane immobilizer molded around the head. PET images were acquired on an ECAT EXACT HR+ (Siemens/CTI, Knoxville Tenn.). After a 10-minute transmission scan, mean 500.71 (SD 160.48) MBq of [^{11}C]-PIB was administered intravenously as a bolus over 30 seconds. Emission data were collected in 3D mode for 90 minutes, binning over 18 frames of increasing duration (3 × 20 sec, 3 × 1 min, 3 × 2 min, 2 × 5 min, and 7 × 10 min). Twenty nine arterial blood samples (each 0.3 ml) were drawn during the scan by pump every 10 sec for 2 min and then every 20 sec for 2 min, followed by manual draws at 6, 12, 20, 30, 40, 50, 60, 80 and 90 min after radioactivity injection. These samples were centrifuged and radioactivity in the plasma measured in the well counter[12]. Images were reconstructed to 128 × 128 matrix (pixel size of 2.5 × 2.5 mm^2). Reconstruction was performed with attenuation correction using the transmission data and scatter correction was done using a model-based approach[28]. The reconstruction filter and estimated image filter were Shepp 0.5 (2.5 full width half maximum (FWHM), Z filter was all pass 0.4 (2.0 FWHM), and the zoom factor was 4.0, leading to a final image resolution of 5.1 mm FWHM at the center of the field of view[29].

Metabolite analyses

The percentage of radioactivity in plasma as unchanged [^{11}C]BTA was determined by HPLC with blood samples taken at 2, 6, 12, 20, 40, 60 and 90 min after radioactivity injection for metabolite analysis. Metabolite and free fractions were collected based on a Bioscan gamma detector and assayed on a Packard Instruments Gamma Counter (Model E5005). All acquired data were subjected to correction for background radioactivity and physical decay to calculate the percentage of the parent compound in the plasma at different time points. In order to reaffirm that the retention time of the parent compound had not shifted during the course of the metabolite analysis, a quality control sample of [^{11}C]BTA was injected at the beginning and the end of the study. The percentage of radioactive parent obtained was used for the measurement of metabolite-corrected arterial input functions.

The ^{18}F-FDG study was conducted one hour after the ^{11}C-PIB scan with the same scanner, scanning mode, positioning, and reconstruction matrix. After a 10-minute transmission scan, a bolus injection of ^{18}F-FDG (mean 178.47 SD 11.92 MBq) was administered intravenously. Emission data were acquired in 3D mode for 60 minutes with 26 frames of increasing duration (8 × 15 sec, 6 × 30 sec, 5 × 1 min, 4 × 5 min, and 3 × 10 min). Thirteen arterial blood samples (each 0.3 ml) were drawn during the scan (by pump every 10 sec for 90 sec and then every 30 sec for 2 min, followed by manual draws at 5, 20, 40 and 60.5 min). These samples were centrifuged and radioactivity in the plasma measured in the well counter[12]. Blood glucose was measured by a glucometer for calculation of the regional cerebral metabolic rate for glucose (rCMRGlu) [30].

Of the 60 subjects, ^{11}C-PIB scans were completed in 58 subjects, of whom 53 subjects had arterial lines. ^{18}F-FDG scans were completed in 56 of the 60 subjects, of whom 52 subjects had arterial lines.

MR Imaging

Magnetic resonance images (MRIs) were acquired using a 1.5T Signa Advantage system (first 17 subjects: 8 CTR, 3 MCI, 6 AD) or a 3T GE scanner (next 42 subjects: 10 CTR, 20 MCI, 12 AD). All scans from the 1.5T scanner were acquired in the coronal plane with the following parameters; 3D spoiled gradient recalled acquisition in the steady state; TR=34 ms, TE=5 ms, FA=45°, 1.5 mm slice thickness (zero gap), 124 slices, FOV 220 mm × 160 mm. All images were reconstructed to a size of 256 × 256 with a resolution of 1.5 × 0.86 × 0.86 mm. Coronal scans from the 3T scanner were acquired with the following parameters; TR= 5.4 ms, TE=2.1 ms, FA=11°, 1 mm slice thickness (zero gap), 160 slices, FOV = 256 mm × 256 mm. All images from the 3T were reconstructed to a size of 256 × 256 with an isotropic resolution of 1 × 1 × 1 mm.

The regions of interest (ROIs) chosen for analysis were based on published studies of ^{11}C-PIB PET and ^{18}F-FDG in cognitively impaired subjects (Table 1). A trained, experienced technician drew the prefrontal, cingulate, parietal cortex, and precuneus (left and right) ROIs using atlas based approaches[31] on MRI scans[10, 32]. The technician also drew the anatomical boundaries for the hippocampus and parahippocampal gyrus, using reliable, published methods[33]. ROIs were transferred to motion-corrected and MRI coregistered PET images.

Image Analysis Platform

Image analysis was performed using Matlab 2006b (The Mathworks, MA) with calls to the following open source packages; Functional Magnetic Resonance Imaging of the Brain's Linear Image Registration Tool (FLIRT) v5, Brain Extraction Tool (BET) v1.2, and University College of London's Statistical Parametric Mapping (SPM5) normalization and segmentation routines. Partial volume correction was not done in this study.

PET Image Processing

To correct for subject motion, de-noising filter techniques were applied to all PET images starting at frame five (2.5 min for ^{11}C-PIB, 1.1 min for ^{18}F-FDG). Frame 8 (5.0 min for ^{11}C-PIB, 1.9 min for ^{18}F-FDG) was the reference to which all other frames were aligned using rigid body FLIRT. The mean of the motion corrected frames was registered, using FLIRT, to each subject's BET skull stripped MRI. The resultant transform was applied to the entire motion-corrected PET dataset.

^{11}C-PIB kinetic analysis

The cerebellum is nearly devoid of amyloid plaques in post-mortem analysis of patients with AD[34] and cerebellar gray matter shows little ^{11}C-PIB retention in CTR and AD[3]. Therefore,

a ROI that included the entire cerebellum was drawn on the MRI. A binary mask of this ROI was created. To correct the cerebellar ROI to include gray matter only, unprocessed MRI images were segmented using SPM5 to derive the probabilistic gray matter (GM_p) map. The gray matter map and all individual PET frames were multiplied (masked) by the cerebellar binary mask. On a frame-by-frame basis, the sum of all voxels in each masked PET image was divided by the sum of all voxels in the masked gray matter map to derive the gray matter cerebellar time activity curve.

^{11}C-PIB (BP_{ND}) PET Modeling

In the 58 subjects who completed the ^{11}C-PIB scan, BP_{ND} was calculated for each ROI using the Logan graphical method[35] from 90-minute PET data, using the gray matter probability corrected time activity curve of the cerebellum as reference (primary analyses for generalizability). The Logan method is stable, has high test-retest reliability[36], and is sensitive to small changes in ^{11}C-PIB when compared to quantification using an arterial input function[37]. In this study, binding potential (BP_p) was also calculated using the Logan graphical method with an arterial input function (n=53, secondary analyses).

^{18}F-FDG kinetic analysis

For comparability to the ^{11}C-PIB analyses, the rCMRGlu ratio of each ROI to cerebellum (sum of 40-60 min mean activity) was used (primary analyses for generalizability). In addition, arterial input function corrected data were also evaluated (secondary analyses).

^{18}F-FDG data were evaluated by a two-tissue compartment model relating the concentration of free ^{18}F-FDG and ^{18}F-FDG-6-PO_4 in the tissue to the ^{18}F-FDG concentration in plasma through four rate constants $k_1^* - k_4^*$ [38]. The estimates of these rate constants obtained by using the classical iterative nonlinear least squares approach are expected to have optimal statistical accuracy in conjunction with a library of functions of the type $e^{-\theta_k t} \otimes c_p^*(t)$ for a range of θ_k values. For the ^{18}F-FDG two-tissue compartment model, each noisy TAC curve is regressed on each possible pair of library functions, the smallest sum of weighted squared errors determining the final fit. The limitations of such an approach are that estimation can be negatively affected by poor choices for θ_k settings, and that estimation of time constants is not as precise as when parameters are estimated iteratively[32]. However, an opportune choice of the θ_k settings is able to obtain estimates of the parameters comparable to those by the standard iterative approach. Furthermore, the rCMRGlu values calculated by using the non-iteratively estimated rate constants are significantly less biased than those obtained by the widely adopted and computationally efficient Patlak graphical approach, which underestimates rCMRGlu due to the assumption of $k_4^*=0$.

Statistical Analyses

Descriptive statistics were used to compare the demographic and clinical variables for the three groups of subjects (CTR, MCI, AD). For ^{11}C-PIB BP_{ND} (binding potential, cerebellar reference), separate ANOVAs were conducted on each ROI with subject group as the between subject factor. Similar ANCOVAs were conducted with age as covariate. Significant main effects in ANOVA were followed up with two-tailed t-tests for post hoc pair-wise comparisons. For the AD-CTR comparison, Cohen's *d* (effect size) was calculated. A similar set of analyses was conducted for ^{18}F-FDG rCMRGlu.

The mean of all the ROIs for BP_{ND} and rCMRGlu were evaluated in separate ANOVAs with subject group as the between subject factor. Significant main effects were followed up with two-tailed t-tests for post hoc pair-wise comparisons. Across the entire sample,

Spearman correlation coefficients between the ROI indices (BP_{ND} or rCMRGlu) in each region and the cognitive assessment measures (MMSE, SRT, ADAS-cog) were examined.

To evaluate the comparative utility of ^{11}C-PIB BP_{ND} and ^{18}F-FDG rCMRGlu, receiver operating characteristic (ROC) analyses were conducted to compare their classification accuracy measured by the area under the curve (AUC) with posthoc calculation of sensitivity and specificity. To distinguish diagnostic groups on each ROI, bivariate linear models were applied to the BP_{ND} and rCMRGlu measures (converted to z-scores) to test whether the measures differed by diagnostic group after controlling for age, and to test whether the group differences were the same for the two standardized measures. Model parameters were estimated with generalized estimating equations to use all available data and account for within-subject correlation between the two measures.

Apolipoprotein E genotyping was not done in the majority of subjects, and hence was not analyzed.

When pair-wise comparisons were made among three diagnostic groups, the alpha criterion for statistical significance was set conservatively at 0.0167 (0.05/3). Significance levels between 0.02 and 0.05 are reported as trend-level effects.

RESULTS

The sample of 60 subjects comprised 18 CTR, 24 MCI and 18 AD patients. On average, subjects had high education levels and were around 70 years old (Table 2). The three groups differed in cognitive test performance on each of the three cognitive tests evaluated in all subjects (AD worse than MCI worse than CTR). Seventeen of 18 AD patients, 5 of 24 MCI patients and no control subjects were receiving acetylcholinesterase inhibitors or memantine.

^{11}C-PIB BP_{ND} (n=58, cerebellar reference)

Across the entire sample, there were no associations between age, sex, education and BP_{ND} in any ROI (Table 3), and no associations in patients between the use of cholinesterase inhibitors/memantine and BP_{ND}. There were strong inverse correlations between BP_{ND} in the prefrontal, cingulate, parietal and precuneus regions and the cognitive test scores across the entire sample (Table 3). These correlations appeared to be driven by group differences, because they were not as strong when examined within each diagnostic group, partly because of some overlap in BP_{ND} values and the restricted range in cognitive scores within each diagnostic group.

In separate ANOVAs on each ROI with subject group (CTR, MCI, AD) as the between subject factor, the three subject groups differed significantly in BP_{ND} in prefrontal cortex ($F=21.9$, $p < .001$), cingulate ($F=13.2$, $p < .001$), parietal cortex ($F=20.1$, $p < .001$), precuneus ($F=28.7$, $p < .001$) and parahippocampal gyrus ($F=6.2$, $P=0.004$) but not in hippocampus ($F=0.4$, $p=0.7$). In ANCOVA on each ROI with subject group (CTR, MCI, AD) as the between subject factor, age was not a significant covariate in any analysis.

In posthoc t-tests, BP_{ND} was higher in AD patients compared to CTR in prefrontal cortex ($t=6.5$, $p < .0001$), cingulate ($t=4.9$, $p < .001$), parietal cortex ($t=6.1$, $p < .0001$), precuneus ($t=7.2$, $p < .0001$) and parahippocampal gyrus ($t=3.4$, $p=0.001$), but not in the hippocampus ($t=0.3$, $p=0.8$). In precuneus and prefrontal cortex, only one control showed BP_{ND} in the AD range and only one AD patient showed BP_{ND} in the control range (Figure 1). BP_{ND} was also higher in AD compared to MCI patients in prefrontal cortex ($t=4.5$, $p < .0001$), cingulate ($t=3.9$, $p=.0003$), parietal cortex ($t=4.8$, $p < .0001$), and precuneus ($t=5.8$, $p < .0001$), with an increase in parahippocampal gyrus ($t=2.7$, $p=0.01$) and no difference in hippocampus ($t=0.5$,

p=0.62). In MCI compared to CTR, BP_{ND} was higher in prefrontal cortex (t=2.3, p=0.02) and there were no significant differences in any of the other five regions. As seen in Figure 1, amnestic MCI patients were similar to AD patients and had non-significantly higher BP_{ND} than non-amnestic MCI patients (n=5) and CTR subjects in several ROIs. The small number of subjects, particularly in the non-amnestic MCI subsample (n=5), likely explains the lack of significance in the MCI subgroup comparisons.

For the AD-CTR comparison, the effect size for BP_{ND} was large (> 2 SD) for several regions, including precuneus (Cohen's *d*=2.81), parietal cortex (*d*=2.28), and mean BP_{ND} (*d*=2.23).

The results obtained for ^{11}C-PIB by using the arterial input function (n=53) led to very similar results with nearly identical significance levels for all comparisons (data available upon request) relative to those obtained using the cerebellar reference data.

^{18}F-FDG PET (n=56, ratio to cerebellum)

Across the entire sample, sex, age and education were unrelated to rCMRGlu in any ROI (Table 4). rCMRGlu in the parietal cortex and precuneus correlated strongly with cognitive test scores across the entire sample, with somewhat weaker correlations between rCMRGlu in the hippocampus and cognitive test scores (Table 4). rCMRGlu values did not differ between patients who did and did not receive cholinesterase inhibitors or memantine.

In ANOVAs on each ROI, rCMRGlu differed across the three subject groups in parietal cortex (F=18.4, p<0.0001), precuneus (F=16.8, p<0.0001) and cingulate (F=5.48, p=0.007), but not the prefrontal cortex (F=0.9, p=0.40), parahippocampal gyrus (F=1.0, p=0.39) or hippocampus (F=1.7, p=0.20). In ANCOVA on each ROI, age was not a significant covariate for any region.

In posthoc t-tests, rCMRGlu was lower in AD patients compared to CTR in parietal cortex (t=5.5, p<0.0001), precuneus (t=5.2, p < 0.0001) and cingulate (t=3.1, p=0.004), but not in other regions. rCMRGlu was lower in AD compared to MCI patients in parietal cortex (t=5.2, p < 0.0001), precuneus (t=5.0, p<0.0001) and cingulate (t=2.7, p=0.008), but not in other regions. rCMRGlu showed no significant differences between MCI (total MCI or amnestic MCI) and control subjects in any ROI. rCMRGlu did not differ significantly between amnestic MCI and non-amnestic MCI patients in any ROI, primarily because the small number of non-amnestic MCI patients (n=5) limited statistical power (Figure 2).

For the AD-CTR comparison, for rCMRGlu the effect size (Cohen's *d*) was 1.59 for precuneus, 1.72 for parietal cortex, and 1.22 for mean value.

Arterial input function derived rCMRGlu analyses (n=52, absolute quantification)

These analyses revealed similar but slightly weaker results to those obtained by using the cerebellar ratio. rCMRGlu was lower in AD compared to CTR in parietal cortex (t=3.0, p=0.006) and precuneus (t=3.3, p=0.003), tended to be lower in cingulate (t=2.1, p < 0.04), and did not differ in prefrontal cortex, parahippocampal gyrus and hippocampus. rCMRGlu tended to be lower in AD compared to MCI patients in parietal cortex (t=2.1, p=0.04) and precuneus (t=2.4, p=0.02), but not in prefrontal cortex (t=0.50, p=0.6), cingulate (t=1.2, p=0.25), parahippocampal gyrus (t=0.0, p=0.97) and hippocampus (t=0.90, p=0.4). rCMRGlu showed no significant differences in any ROI between MCI and control subjects, or between amnestic and non-amnestic MCI patients.

Mean ROI (^{11}C-PIB BP_{ND} and ^{18}F-FDG rCMRGlu)

In ANOVA on the unweighted mean of all the ROIs examined, the three subject groups differed significantly in ^{11}C-PIB BP_{ND} (F=19.6, P < .0001) and rCMRGlu (F=9.2, p=0.0004). Mean ^{11}C-PIB BP_{ND} was higher in AD compared to CTR (t=6.0, p < .0001) and AD compared to MCI (t=4.7, p < .0001), but not MCI compared to CTR (t=1.6, p=0.11). Mean rCMRGlu was higher in AD compared to CTR (t=3.9, p=.0003) and AD compared to MCI (t=3.7, p=.0005), but not MCI compared to CTR (t=0.4, p=0.66). In ANCOVA on mean ^{11}C-PIB BP_{ND}, the groups differed significantly (F=19.2, p < .0001) and age was not a significant covariate (F=0.01, p=0.9). In ANCOVA on mean rCMRGlu in the three subject groups, the groups differed significantly (F=9.2, p=0.0004) and age was not a significant covariate (F=0.53, p=0.47).

^{11}C-PIB with ^{18}F-FDG correlations

Spearman correlation coefficients between ^{11}C-PIB BP_{ND} and rCMRGlu within each ROI ranged from −0.01 to −0.4 and the correlation between mean ROI values was −0.13, indicating relative dissociation between the ^{11}C-PIB and ^{18}F-FDG measures.

Comparative utility of ^{11}C-PIB BP_{ND} and ^{18}F-FDG rCMRGlu

For BP_{ND}, the most prominent difference between AD and CTR was in precuneus, consistent with the literature (Figures 1 and 3). For rCMRGlu, the most prominent difference between AD and CTR was in parietal cortex, consistent with the literature (Figures 2 and 3). In the sample of 16 AD and 17 CTR subjects (total n=33) who had both PET scans, based on the predicted probability of an AD diagnosis using separate logistic regression models, for precuneus BP_{ND} estimated AUC=0.938 and parietal cortex rCMRGlu estimated AUC=0.915. Combining these two PET measures led to an estimated AUC=0.989. For the same AD-CTR comparison, for mean BP_{ND} estimated AUC=0.923 was non-significantly higher than for mean rCMRGlu estimated AUC=0.800.

To evaluate sensitivity and specificity for BP_{ND} in precuneus and rCMRGlu in parietal cortex, ROC analyses were used to derive the cutoff points that maximized the product of sensitivity and specificity. For the precuneus BP_{ND} cut-point of 0.4087 (values above this considered abnormal), for AD versus CTR sensitivity was 0.944 and specificity was 0.944, and for MCI versus CTR sensitivity was 0.273 and specificity was 0.944. For the mean BP_{ND} cut-point of 0.1948 (values above this considered abnormal), for AD versus CTR sensitivity was 0.944 and specificity was 0.944, and for MCI versus CTR sensitivity was 0.273 and specificity was 0.944. For the parietal cortex rCMRGlu cut-point of 1.0301 (values below this considered abnormal), for AD versus CTR sensitivity was 0.875 and specificity was 0.882, and for MCI versus CTR sensitivity was 0.174 and specificity was 0.882. For the mean rCMRGlu cut-point of 0.9574 (values below this considered abnormal), for AD versus CTR sensitivity was 0.813 and specificity was 0.706, and for MCI versus CTR sensitivity was 0.217 and specificity was 0.706.

In comparing diagnostic group differences in BP_{ND} to diagnostic group differences in rCMRGlu, bivariate linear models controlling for age were applied to the PET regional measures (converted to z-scores). In distinguishing AD from CTR, BP_{ND} was significantly better than rCMRGlu only in prefrontal cortex (p=0.015) mainly because prefrontal cortex rCMRGlu did not differ in the two diagnostic groups (p=0.42). Mean BP_{ND} was not significantly better than mean rCMRGlu in classifying AD versus CTR (p=0.37). BP_{ND} was not significantly different from rCMRGlu in distinguishing AD from MCI or MCI from CTR in any region or mean values.

DISCUSSION

^{11}C-PIB BP_{ND} was higher in AD patients compared to CTR with a large effect size for precuneus, parietal cortex and mean values. There was near-complete separation in precuneus, which appears to be the region most likely to show differences between AD and CTR[10]. ^{11}C-PIB BP_{ND} was also higher in AD compared to CTR in prefrontal and cingulate cortex but not in the hippocampus, consistent with the literature[3, 9, 11]. These findings support the relative regional distribution of amyloid reported in other ^{11}C-PIB studies that also found increased prefrontal, parietal and precuneus uptake[3, 9] and is consistent with autopsy data showing that in early AD, amyloid deposition is greater in the frontal and parietal cortex than the hippocampus[5]. In the ROIs examined, ^{11}C-PIB BP_{ND} differences occurred in AD compared to CTR, and AD compared to MCI. MCI differed significantly from CTR only in prefrontal cortex [15, 39, 40, 41, 18]. Based on the cutoff value used in this study, the majority of MCI patients had BP_{ND} like controls and a minority had BP_{ND} like AD patients. Possible explanations are the inclusion of non-amnestic MCI patients (n=5, of whom 4 scored below the cutoff in parietal cortex and precuneus) in the MCI sample, and the fact that approximately one-third of the MCI sample had been followed in the clinic for 1-2 years without conversion to dementia. The latter group would be less likely to have AD brain pathology than MCI patients who present for initial evaluation.

Controls with high ^{11}C-PIB retention were rare in our sample, with little overlap between AD and CTR in precuneus and prefrontal cortex (Figure 1). In contrast, other reports show high ^{11}C-PIB retention in approximately 20% of healthy elderly control subjects[10]. Different criteria used to select control subjects may partly account for these differences across studies. In our study, impairment on neuropsychological tests was a strict exclusion criterion for healthy control subjects, in contrast to the use of the Clinical Dementia Rating of global cognitive/functional ability in some studies that may have allowed for the inclusion of control subjects with mild neuropsychological deficits.[10] Initial follow-up studies suggest that increased ^{11}C-PIB retention is associated with an increased likelihood of healthy controls converting to MCI, and MCI patients converting to AD[14, 18]. In a recent study, PIB-positive patients with MCI were more likely to convert to AD than PIB-negative patients, and faster converters had higher PIB retention levels at baseline than slower converters[19]. In patients diagnosed with AD, there may be no increase[42] or a small increase in ^{11}C-PIB retention during follow-up[43, 39].

^{18}F-FDG rCMRGlu differed among the three subject groups in the precuneus, parietal cortex, and cingulate, but not in the prefrontal cortex, hippocampus and parahippocampal gyrus. These findings were confined to the AD-CTR and AD-MCI comparisons, and MCI-CTR comparisons were not significant. The findings are consistent with the literature on parietal and posterior cingulate metabolic deficits distinguishing AD from CTR, but in this sample there were no significant differences in medial temporal regions. Other reports indicate that both parietal and temporal metabolic deficits distinguish AD from CTR[20]. We observed few MCI-CTR differences, but another report in a small sample suggests that regional decrease in rCMRGlu in parietal and posterior cingulate may be superior to ^{11}C-PIB in distinguishing MCI from CTR[24]. Although there were no associations for rCMRGlu measures with age in this sample, changes are known to occur with aging in AD patients, with younger AD patients clearly showing the typical parietotemporal hypometabolism while older AD patients have a more global reduction in glucose metabolism[20].

When both BP_{ND} and rCMRGlu were compared directly, BP_{ND} was marginally, but non-significantly, superior to rCMRGlu in distinguishing AD from CTR and AD from MCI. Figure 3 shows that there are visible uptake differences and different patterns of uptake across the three groups using the two tracers. The AUC analysis on an ROI level showed

strong utility for BP_{ND} and possibly greater utility for the combination of BP_{ND} and rCMRGlu, and this approach may have potential for better segregating patient populations and predicting conversion to AD in longitudinal studies of patients with MCI. Alternative assessments include total cortical binding[10] or visual assessment by a radiologist[11], both of which have shown moderate to strong sensitivity and specificity in separating AD from CTR but less information is available on the use of these approaches in MCI. With respect to structural imaging, regional PIB retention and MRI hippocampal atrophy may provide complementary information in MCI and AD[16]. Of note, approximately 5-10% of patients diagnosed as AD in an academic specialty center, as in this study, do not have AD when patients are followed to autopsy[2].

^{11}C-PIB retention in several regions showed strong inverse correlations with cognitive measures across the sample, consistent with some studies in patients with MCI and AD[44, 45] and elderly subjects with cognitive decline[14], but not all studies show such strong correlations[13, 16]. ^{18}F-FDG rCMRGlu in the parietal cortex and precuneus showed the strongest correlations with cognitive measures, and rCMRGlu in the hippocampus also showed significant correlations with some cognitive measures. These correlations were not as strong when examined within each diagnostic group, partly because of some overlap in BP_{ND} values and the restricted range in cognitive scores within each diagnostic group.

These neuroimaging-clinical associations are consistent with the parietal, temporal and posterior cingulate pathology known to occur in AD[4].

For ^{11}C-PIB, results using the Logan method and a cerebellar reference region were very similar to those obtained utilizing the arterial input function, supporting other work indicating that an arterial line may not be necessary for ^{11}C-PIB scans[37]. Further, the FDG results using a region of interest to cerebellar ratio in order to provide direct comparability to the ^{11}C-PIB analyses[24] were as strong or stronger than those obtained with the arterial input function and absolute quantification, supporting the use of this analytic approach in MCI and mild AD. Visual reads or voxel-based statistical approaches may be more efficient than ROI methods for ^{18}F-FDG analyses when used for other purposes.

Limitations included the lack of apolipoprotein E genotyping in the majority of subjects; the presence of the apo E e4 allele has been shown to be associated with increased PIB retention[46,47]. The study was cross-sectional and follow-up data to examine the prognostic implications of the baseline PET findings are clearly needed.

Conclusion

^{11}C-PIB PET BP_{ND} strongly distinguished diagnostic groups, and when combined with ^{18}F-FDG PET rCMRGlu this effect became stronger suggesting that the two techniques provide complementary information. The results of this study and the literature suggest that the potential added value of complementary PET techniques to the information obtained from clinical evaluation and neuropsychological testing needs to be clarified in longitudinal studies. Although amyloid deposition in the brain is known to occur very early in AD, it remains unclear if ^{11}C-PIB PET shows increased retention before ^{18}F-FDG PET shows decreased rCMRGlu prior to the clinical diagnosis of AD[41,43]. Further, the potential of ^{11}C-PIB PET as a surrogate marker in clinical trials, particularly of anti-amyloid agents, needs to be established.

Acknowledgments

This study was supported by research support from GlaxoSmithKline (GSK) and a grant from the National Institute of Aging (R01AG17761).

REFERENCES

1. Miniño AM, Heron MP, Murphy SL, et al. Centers for Disease Control and Prevention National Center for Health Statistics National Vital Statistics System. Deaths: final data for 2004. Natl Vital Stat Rep. Aug 21; 2007 55(19):1–119.
2. Knopman DS, DeKosky ST, Cummings JL, et al. Practice parameter: diagnosis of dementia (an evidence-based review). Report of the Quality Standards Subcommittee of the American Academy of Neurology. Neurology. 2001; 56(9):1143–53. [PubMed: 11342678]
3. Klunk WE, Engler H, Nordberg A, et al. Imaging brain amyloid in Alzheimer's disease with Pittsburgh Compound-B. Ann Neurol. Mar; 2004 55(3):306–19. [PubMed: 14991808]
4. Hyman BT, West HL, Rebeck GW, et al. Quantitative analysis of senile plaques in Alzheimer disease: observation of log-normal size distribution and molecular epidemiology of differences associated with apolipoprotein E genotype and trisomy 21 (Down syndrome). Proc Natl Acad Sci U S A. Apr 11; 1995 92(8):3586–90. [PubMed: 7724603]
5. Price JL, Morris JC. Tangles and plaques in nondemented aging and "preclinical" Alzheimer's disease. Ann Neurol. 1999; 45:358–368. [PubMed: 10072051]
6. Mathis CA, Lopresti BJ, Klunk WE. Impact of amyloid imaging on drug development in Alzheimer's disease. Nucl Med Biol. Oct; 2007 34(7):809–22. [PubMed: 17921032]
7. Bacskai BJ, Frosch MP, Freeman SH, et al. Molecular imaging with Pittsburgh Compound B confirmed at autopsy: a case report. Arch Neurol. Mar; 2007 64(3):431–4. [PubMed: 17353389]
8. Ikonomovic MD, Klunk WE, Abrahamson EE, et al. Post-mortem correlates of in vivo PiB-PET amyloid imaging in a typical case of Alzheimer's disease. Brain. Jun; 2008 131(Pt 6):1630–45. [PubMed: 18339640]
9. Rowe CC, Ng S, Ackermann U, et al. Imaging beta-amyloid burden in aging and dementia. Neurology. May 15; 2007 68(20):1718–25. [PubMed: 17502554]
10. Mintun MA, Larossa GN, Sheline YI, et al. Morris JC. [11C]PIB in a nondemented population: potential antecedent marker of Alzheimer disease. Neurology. Aug 8; 2006 67(3):446–452. [PubMed: 16894106]
11. Ng S, Villemagne VL, Berlangieri S, et al. Visual assessment versus quantitative assessment of 11C-PIB PET and 18F-FDG PET for detection of Alzheimer's disease. J Nucl Med. 2007; 48(4): 547–552. [PubMed: 17401090]
12. Mikhno A, Devanand D, Pelton G, et al. Voxel-based analysis of 11C-PIB scans for diagnosing Alzheimer's disease. J Nucl Med. Aug; 2008 49(8):1262–9. [PubMed: 18632806]
13. Aizenstein HJ, Nebes RD, Saxton JA, et al. Frequent amyloid deposition without significant cognitive impairment among the elderly. Arch Neurol. Nov; 2008 65(11):1509–17. [PubMed: 19001171]
14. Villemagne VL, Pike KE, Darby D, et al. Abeta deposits in older non-demented individuals with cognitive decline are indicative of preclinical Alzheimer's disease. Neuropsychologia. 2008; 46(6):1688–97. [PubMed: 18343463]
15. Forsberg A, Engler H, Almkvist O, et al. PET imaging of amyloid deposition in patients with mild cognitive impairment. Neurobiol Aging. Oct; 2008 29(10):1456–65. [PubMed: 17499392]
16. Jack CR Jr, Lowe VJ, Senjem ML, et al. 11C PiB and structural MRI provide complementary information in imaging of Alzheimer's disease and amnestic mild cognitive impairment. Brain. Mar; 2008 131(Pt 3):665–80. [PubMed: 18263627]
17. Kemppainen NM, Aalto S, Wilson IA, et al. PET amyloid ligand [11C]PIB uptake is increased in mild cognitive impairment. Neurology. May 8; 2007 68(19):1603–6. [PubMed: 17485647]
18. Wolk DA, Price JC, Saxton JA, et al. Amyloid imaging in mild cognitive impairment subtypes. Ann Neurol. May; 2009 65(5):557–68. [PubMed: 19475670]
19. Okello A, Koivunen J, Edison P, et al. Conversion of amyloid positive and negative MCI to AD over 3 years: an 11C-PIB PET study. Neurology. Sep 8; 2009 73(10):754–60. [PubMed: 19587325]
20. Silverman DH, Small GW, Chang CY, et al. Positron emission tomography in evaluation of dementia: Regional brain metabolism and long-term outcome. JAMA. 2001; 286:2120–2127. [PubMed: 11694153]

21. Mosconi L, Tsui WH, Herholz K, et al. Multicenter standardized 18F-FDG PET diagnosis of mild cognitive impairment, Alzheimer's disease, and other dementias. J Nucl Med. Mar; 2008 49(3): 390–8. [PubMed: 18287270]
22. Chételat G, Desgranges B, de la Sayette V, et al. Mild cognitive impairment: Can FDG-PET predict who is to rapidly convert to Alzheimer's disease? Neurology. Apr 22; 2003 60(8):1374–7. [PubMed: 12707450]
23. Drzezga A, Lautenschlager N, Siebner H, et al. Cerebral metabolic changes accompanying conversion of mild cognitive impairment into Alzheimer's disease: a PET follow-up study. Eur J Nucl Med Mol Imaging. Aug; 2003 30(8):1104–13. [PubMed: 12764551]
24. Li Y, Rinne JO, Mosconi L, et al. Regional analysis of FDG and PIB-PET images in normal aging, mild cognitive impairment, and Alzheimer's disease. Eur J Nucl Med Mol Imaging. Jun 20.2008
25. McKhann G, Drachman D, Folstein M, et al. Clinical diagnosis of Alzheimer's disease: report of the NINCDS-ADRDA Work Group under the auspices of Department of Health and Human Services Task Force on Alzheimer's Disease. Neurology. 1984; 34(7):939–944. [PubMed: 6610841]
26. Petersen RC, Smith GE, Waring SC, et al. Mild cognitive impairment: clinical characterization and outcome. Arch Neurol. Mar; 1999 56(3):303–8. Mild cognitive impairment: clinical characterization and outcome. *Erratum in Arch Neurol*;56(6):760. [PubMed: 10190820]
27. Parsey RV, Sokol LO, Bélanger MJ, Kumar JS, Simpson NR, Wang T, Pratap M, Van Heertum RL, John Mann J. Amyloid plaque imaging agent [C-11]-6-OH-BTA-1: biodistribution and radiation dosimetry in baboon. Nucl Med Commun. Oct; 2005 26(10):875–880. [PubMed: 16160646]
28. Watson CC, Casey ME. A single scatter simulation technique for scatter correction in 3D PET. Dordrecht. 1996 ND.
29. Mawlawi O, Martinez D, Slifstein M, et al. Imaging human mesolimbic dopamine transmission with positron emission tomography: I. Accuracy and precision of D(2) receptor parameter measurements in ventral striatum. J Cereb Blood Flow Metab. Sep; 2001 21(9):1034–1057. [PubMed: 11524609]
30. Deloar HM, Fujiwara T, Shidahara M, et al. Estimation of absorbed dose for 2-[F-18]fluoro-2-deoxy-D-glucose using whole-body positron emission tomography and magnetic resonance imaging. Eur J Nucl Med. Jun; 1998 25(6):565–74. [PubMed: 9618570]
31. Duvernoy, H. The human brain. Surface, three-dimensional sectional anatomy and MRI. Sringer-Verlag Wien; New York: 1991.
32. Ogden RT, Ojha A, Erlandsson K, et al. In vivo quantification of serotonin transporters using [(11)C]DASB and positron emission tomography in humans: modeling considerations. J Cereb Blood Flow Metab. Jan; 2007 27(1):205–17. Epub 2006 May 17. Erratum in: *J Cereb Blood Flow Metab.* Apr;27(4):874. [PubMed: 16736050]
33. Devanand DP, Pradhaban G, Liu X, et al. Hippocampal and entorhinal atrophy in mild cognitive impairment: prediction of Alzheimer disease. Neurology. Mar 13; 2007 68(11):828–36. [PubMed: 17353470]
34. Joachim CL, Morris JH, Selkoe DJ. Diffuse senile plaques occur commonly in the cerebellum in Alzheimer's disease. Am J Pathol. Aug; 1989 135(2):309–319. [PubMed: 2675616]
35. Logan J, Fowler JS, Volkow ND, et al. Distribution volume ratios without blood sampling from graphical analysis of PET data. J Cereb Blood Flow Metab. Sep; 1996 16(5):834–840. [PubMed: 8784228]
36. Price JC, Klunk WE, Lopresti BJ, et al. Kinetic modeling of amyloid binding in humans using PET imaging and Pittsburgh Compound-B. J Cereb Blood Flow Metab. Nov; 2005 25(11):1528–1547. [PubMed: 15944649]
37. Lopresti BJ, Klunk WE, Mathis CA, et al. Simplified quantification of Pittsburgh Compound B amyloid imaging PET studies: a comparative analysis. J Nucl Med. Dec; 2005 46(12):1959–1972. [PubMed: 16330558]
38. Phelps ME, Huang SC, Hoffman EJ, et al. Tomographic measurement of local cerebral glucose metabolic rate in humans with (F-18)2-fluoro-2-deoxy-D-glucose: validation of method. Ann Neurol. Nov; 1979 6(5):371–88. [PubMed: 117743]

39. Forsberg A, Engler H, Almkvist O, et al. PET imaging of amyloid deposition in patients with mild cognitive impairment. Neurobiol Aging. Oct; 2008 29(10):1456–65. [PubMed: 17499392]
40. Raji CA, Becker JT, Tsopelas ND, et al. Characterizing regional correlation, laterality and symmetry of amyloid deposition in mild cognitive impairment and Alzheimer's disease with Pittsburgh Compound B. J Neurosci Methods. 2008; 172(2):277–82. [PubMed: 18582948]
41. Lowe VJ, Kemp BJ, Jack CR Jr, et al. Comparison of 18F-FDG and PiB PET in cognitive impairment. J Nucl Med. Jun; 2009 50(6):878–86. [PubMed: 19443597]
42. Engler H, Forsberg A, Almkvist O, et al. Two-year follow-up of amyloid deposition in patients with Alzheimer's disease. Brain. Nov; 2006 129(Pt 11):2856–66. [PubMed: 16854944]
43. Edison P, Archer HA, Hinz R, et al. Amyloid, hypometabolism, and cognition in Alzheimer disease: an [11C]PIB and [18F]FDG PET study. Neurology. Feb 13; 2007 68(7):501–8. [PubMed: 17065593]
44. Pike KE, Savage G, Villemagne VL, et al. Beta-amyloid imaging and memory in non-demented individuals: evidence for preclinical Alzheimer's disease. Brain. Nov; 2007 130(Pt 11):2837–44. Epub 2007 Oct 10. [PubMed: 17928318]
45. Mormino EC, Kluth JT, Madison CM, et al. Alzheimer's Disease Neuroimaging Initiative. Episodic memory loss is related to hippocampal-mediated beta-amyloid deposition in elderly subjects. Brain. May; 2009 132(Pt 5):1310–23. Epub 2008 Nov 28. [PubMed: 19042931]
46. Drzezga A, Grimmer T, Henriksen G, et al. Effect of APOE genotype on amyloid plaque load and gray matter volume in Alzheimer disease. Neurology. 2009; 72:1487–1494. M. [PubMed: 19339712]
47. Reiman EM, Chen K, Liu X, Bandy D, et al. Fibrillar amyloid-beta burden in cognitively normal people at 3 levels of genetic risk for Alzheimer's disease. Proc Natl Acad Sci U S A. Apr 21; 2009 106(16):6820–5. [PubMed: 19346482]
48. Rabinovici GD, Furst AJ, O'Neil JP, et al. 11C-PIB PET imaging in Alzheimer disease and frontotemporal lobar degeneration. Neurology. Apr 10; 2007 68(15):1205–12. PMID: 17420404. [PubMed: 17420404]
49. Ziolko SK, Weissfeld LA, Klunk WE, et al. Evaluation of voxel-based methods for the statistical analysis of PIB PET amyloid imaging studies in Alzheimer's disease. Neuroimage. Oct 15; 2006 33(1):94–102. [PubMed: 16905334]
50. Jagust WJ, Landau SM, Shaw LM, et al. Alzheimer's Disease Neuroimaging Initiative. Relationships between biomarkers in aging and dementia. Neurology. Oct 13; 2009 73(15):1193–9. PMID: 19822868. [PubMed: 19822868]
51. Drzezga A, Grimmer T, Henriksen G, et al. Imaging of amyloid plaques and cerebral glucose metabolism in semantic dementia and Alzheimer's disease. Neuroimage. Jan 15; 2008 39(2):619–33. [PubMed: 17962045]
52. Kadir A, Andreasen N, Almkvist O, et al. Effect of phenserine treatment on brain functional activity and amyloid in Alzheimer's disease. Ann Neurol. May; 2008 63(5):621–31. [PubMed: 18300284]

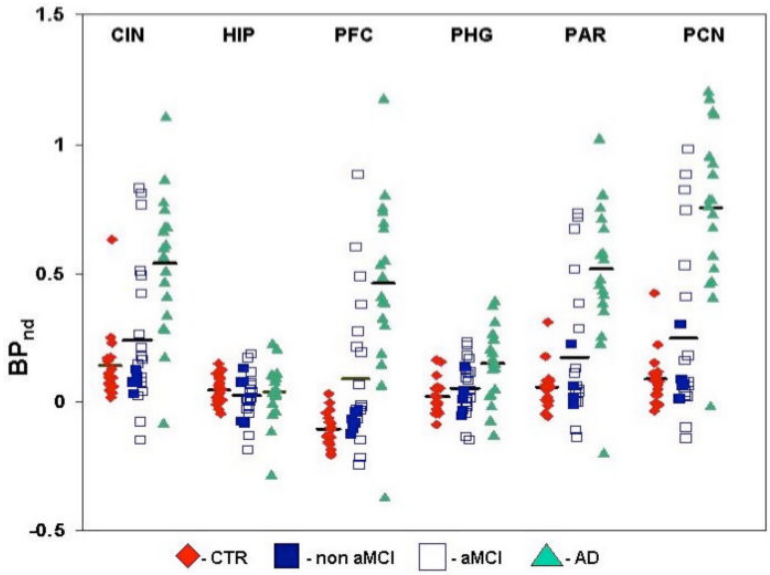

Figure 1.

^{11}C-PIB PET BP_{ND} in Alzheimer's Disease (AD), mild cognitive impairment (MCI), and healthy control subjects (CTR). BP_{ND} data were derived from regional analysis of MR coregistered ^{11}C-PIB images using the Logan method with gray matter cerebellum as the reference region.

CIN=cingulate, HIP=hippocampus, PFC=prefrontal cortex; PHG=parahippocampal gyrus, PAR=parietal cortex, PCN=precuneus. Non aMCI=non-amnestic MCI, aMCI=amnestic MCI.

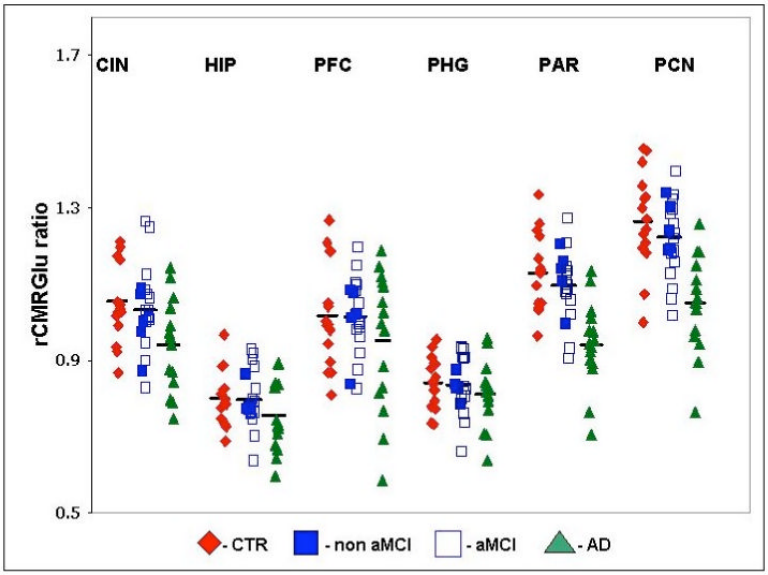

Figure 2.

^{18}F-FDG PET rCMRGlu in Alzheimer's Disease (AD), mild cognitive impairment (MCI), and healthy control subjects (CTR). rCMRGlu was derived from regional analysis of MR coregistered ^{18}F-FDG PET images with ratio of each ROI to cerebellum represented on the y-axis.

Non aMCI=non-amnestic MCI, aMCI=amnestic MCI. CIN=cingulate, HIP=hippocampus, PFC=prefrontal cortex; PHG=parahippocampal gyrus, PAR=parietal cortex, PCN=precuneus.

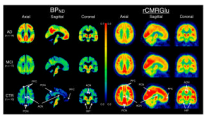

Figure 3.

Comparison of CTR, MCI, and AD subjects' BP_{ND} (left) and rCMRglu (right) data derived from PET ^{11}C-PIB and ^{18}F-FDG scans respectively. All PET data was non-linearly registered, using each individual's MRI, to the SPM5 MNI single subject MRI template using the Automated Registration Toolbox (ART). MNI space BP_{ND} and rCMRGlu maps were averaged voxel-by-voxel in the AD (first row), MCI (second row), and CTR (third row) groups. The middle color bar represents the BP_{ND} (left side) and rCMRglu (right side) value in the images. Arrows point to regions of interest for the prefrontal cortex (PFC), precuneus (PCN), anterior cingulate (ACN), and hippocampus (HIP).

J Geriatr Psychiatry Neurol. Author manuscript; available in PMC 2011 June 8.

Table 1

Published studies examining both ^{11}C-PIB and ^{18}F-FDG PET in samples of AD and controls, or AD and MCI and controls.

Author, year	Sample	PIB	FDG	Analysis Method	Results	Sensitivity, specificity, AUC	Comment
Ziolko et al 2006[49]	10 AD, 11 CTR	Cerebellar reference	Cerebellar reference	MR-PET registration using automated methods for centering and alignment and reslicing; voxel-based analysis and SPM	AD differed from controls in several regions	Not reported	Methods paper
Rabinovici et al 2007[48]	7 AD, 12 FTLD, 8 controls	Distribution volume ratio (DVR) images, cerebellar reference	Summed frames	Visual Rating	PIB + identified 7/7 AD, 4/12 FTLD, 1/8 CTR. FDG discrimination was not strong	PIB positivity and FDG not very specific for FTLD	Use of PIB in distinguishing AD from FTLD is uncertain
Edison et al 2007[43]	14 CTR, 19 AD	PIB ROI ratio to cerebellum	FDG absolute quantification with arterial input function	ROI analyses	PIB increased in AD in several regions and inversely correlated with facial and word recognition tests. Increased PIB uptake correlated with lower rCMRGlc in temporal and parietal cortices.	PIB-PET detected an increased amyloid plaque load in 89% of patients with probable AD	Rigorous methods used
Ng et al 2007[11]	25 CTR, 15 AD	Visual ratings and summed images of SUV data with cerebellar reference. Individualized MRI coregistration.	Visual ratings and cerebellar reference	Visual ratings for both PIB and FDG; quantitative PIB analysis combined SPM and ROI methods (cerebellar reference)	PIB visual better than FDG visual ratings, particularly in older subjects. Quantitative PIB analysis showed 95% accuracy for AD diagnosis. Cohen's effect size 3.87 for PIB and 1.53 for FDG.	Visual rating accuracy around 90% for PIB and 70% for FDG in discriminating AD from CTR.	MCI not studied
Li et al 2008[24]	7 CTR, 13 MCI, 17 AD	Coregistered MNI PET template, then 9 manual	Coregistered MNI PET template, then 9	ROI analyses using cerebellar	ROI findings largely consistent with literature. Hippocampal	The two best measures (HIP MRglc and MFG	FDG suggested to be better than PIB in

Author, year	Sample	PIB	FDG	Analysis Method	Results	Sensitivity, specificity, AUC	Comment
		ROIs using subject's MRI.	manual ROIs using subject's MRI. Cerebellar reference for both PIB and FDG.	reference for both PIB and FDG	metabolism and middle frontal gyrus PIB uptake were the best discriminators of NL from MCI and NL from AD. HIP MRglc and MFG PIB best discriminators; 94% accuracy for AD versus controls but only 54% for MCI versus CTR.	PIB uptake) showed high diagnostic agreement for AD (94%) and poor agreement for MCI (54%). For NL vs. MCI, combining these two measures increased the accuracy for PIB (75%) and for FDG (85%) to 90%.	discriminating MCI and controls; overall findings suggest potential utility of both FDG and PIB.
Forsberg et al 2008[15]	27 AD, 21 MCI, 6 controls	PIB images aligned to the respective FDG images that served as templates. Cerebellar reference region.	Patlak method, arterialized-venous plasma samples. Normalized to pons.	ROI analyses, early and late summation PET images used	PIB: AD showed decreased metabolism in several ROIs but no differences between MCI and CTR. PIB correlated inversely with episodic memory but FDG did not.	Not reported. 7 MCI patients who converted during follow-up to AD showed significantly higher PIB retention compared to non-converting MCI patients.	Follow-up data in MCI subsample suggest that PIB may have predictive utility
Kadir et al 2008[52]	10 AD, 6 CTR, phenserine versus donepezil/placebo trial	ROIs, cerebellar reference	Venous arterialized samples, Patlak method, normalized to pons	ROI for PIB, venous arterialized blood samples and Patlak Method for FDG	Significant correlations between rCMRglc in parietotemporal region and composite neuropsychological z score	Not provided, pre-post change and not baseline was the focus in this clinical trial	Small sample, no MCI subjects

Author, year	Sample	PIB	FDG	Analysis Method	Results	Sensitivity, specificity, AUC	Comment
Drzezga et al 2008[51]	8 AD, 8 semantic dementia (FTLD), 8 historical controls	SUVR, cerebellar reference, PVC applied	SPM, MNI and Tailarach space, PVC applied	Volume-of-interest analysis (VOI), cerebellar reference, and voxel-based statistical group comparisons (SPM2)	Significant differences for PIB in all regions, largest in temporal cortex and least in occipital cortex. FDG showed decreased uptake in parietal region only	Not provided	Small sample, MCI not studied
Jagust et al 2009[50]	10 AD, 11 controls, 34 MCI	SUVR normalized to cerebellum, ROIs drawn on MR template. Mean cortical PIB SUVR used.	MNI MRI template, referenced to average of pons and cerebellar vermis. Mean ROI value used.	Compared classification using cut-points and kappa coefficients.	PIB + associated with CSF biomarkers but not to cognition. FDG less related to CSF biomarkers but better to cognition.	Not reported	Focus on relation to biomarkers and not PIB/FDG comparison to distinguish subject groups
Lowe et al 2009[41]	20 CTR, 17 aMCI, 6 naMCI, 13 AD. 2 PET scanners used, no arterial lines. PVC and non-PVC data presented.	PIB normalized to cerebellum. Cortical ratio and SUV used.	FDG normalized to pons. Cortical ratio and SUV used.	Global measures only; PIB separated naMCI and aMCI.	PIB similar to FDG in discriminating groups but only PIB showed significant separation of amnestic and nonamnestic MCI groups.	Likelihood of diagnosis based on 25th and 75th percentile for PIB and FDG presented. Results similar to current study.	Similar diagnostic accuracy overall but findings indirectly suggest early amyloid deposition before cerebral metabolic reductions in MCI

Table 2

Demographic and Cognitive Characteristics of the Sample.

Variable	Total n=60	Control n=18	MCI n=24	AD N=18
Sex (% female)	55.0	55.5	50.0	61.1
Age at scan	68.7 (8.8)	68.5 (9.4)	69.5 (9.2)	67.9 (8.1)
Education (years)	16.91 (2.7)	17.4 (2.3)	17.4 (2.7)	15.7 (2.8)
MMSE total score	26.3 (3.6)	28.7 (0.9)	27.8 (1.6)	21.8 (3.2)
SRT total score	41.2 (13.8)	53.1 (8.1)	42.9 (10.5)	27.7 (9.9)
SRT delayed recall	5.0 (3.6)	8.7 (1.7)	4.9 (3.1)	1.6 (1.9)
ADAS-Cog total score	8.2 (4.8)	4.0 (1.9)	6.8 (2.0)	13.9 (3.9)

All values are means (standard deviations), or percentages.

MMSE: Folstein Mini-Mental State Exam, range 0-30.

SRT: Selective Reminding Test, 12-item, 6-trial version.

ADAS-Cog: Alzheimer's Disease Assessment Scale-Cognition.

Table 3

Spearman correlation coefficients between ^{11}C-PIB regional binding potential (BP_{ND}, cerebellar reference) and demographic/cognitive measures (n=58).

Variable	Prefrontal Cortex	Cingulate	Parahippocampal gyrus	Hippocampus	Parietal cortex	Precuneus
Age	−.05 p=0.73	.09 p=0.50	.07 p=0.59	−.06 p=0.64	−.00 p=0.98	−.04 p=0.77
Education	−.21 p=0.11	−.07 p=0.61	.08 p=0.56	0.09 p=0.50	−0.06 p=0.64	−0.13 p=0.32
MMSE	−0.51 p < .001	−0.45 p<.001	−0.24 p=0.07	0.10 p=0.45	−0.43 p< .001	−0.44 p< .001
ADAS-cog	0.63 p<0.001	.51 p < .001	0.32 p=0.02	0.01 p=0.96	0.52 p<.001	0.58 p<.001
SRT total recall	−0.56 p < .001	−0.42 p=.001	−0.20 p=0.13	0.03 p=0.82	−0.41 p=.002	−0.45 p< .001
SRT delayed recall	−0.66 p < .001	−0.48 p < .001	−0.29 p=0.03	−0.00 p=0.99	−0.50 p< .001	−0.55 p< .001

Table 4

Spearman correlation coefficients between ^{18}F-FDG rCMRGlu (ratio of region of interest to cerebellum) and demographic/cognitive measures (n=56).

Variable	Prefrontal Cortex	Cingulate	Parahippocampal gyrus	Hippocampus	Parietal cortex	Precuneus
Age	−0.11 p=0.42	−0.16 p=0.23	−0.19 p=0.15	−0.13 p=0.33	−0.02 p=0.87	0.05 p=0.73
Education	−0.14 p=0.29	−0.05 p=0.70	−0.02 p=0.86	0.06 p=0.65	0.05 p=0.71	0.01 p=0.95
MMSE	0.09 p=0.52	0.32 p=0.02	0.34 p=0.01	0.37 p=0.005	0.65 p < .001	0.62 p<.001
ADAS-cog	0.00 p=1.00	−0.17 p=0.22	−0.14 p=0.30	−0.18 p=0.18	−0.49 p<.001	−0.43 p=.001
SRT total recall	0.02 p=0.91	0.18 p=0.17	0.20 p=0.14	0.27 p=0.04	0.44 p<.001	0.40 p=.002
SRT delayed recall	−0.04 p=0.80	0.19 p=0.16	0.29 p=0.03	0.30 p=0.02	0.43 p=.001	0.39 p=.003